Structural Identification of a Concrete-Filled Steel Tubular Arch Bridge via Ambient Vibration Test Data

Yun Zhou, Ph.D.[1]; Junkai Zhang[2]; Weijian Yi, Ph.D.[3]; Yunzhong Jiang[4]; and Qin Pan, Ph.D.[5]

Abstract: Structural identification (St-Id) is an effective structural evaluation approach for health monitoring and performance-based engineering. However, various uncertainties may significantly influence the reliability of St-Id. This paper presents ambient vibration measurements to develop a baseline model for a newly constructed arch bridge over Hongshui River in Guangxi, China. In this study, modal parameter identification was performed using the random decrement (RD) technique together with the complex mode indicator function (CMIF) algorithm, and the results were compared with those from stochastic subspace identification (SSI). First, a three-dimensional (3D) finite-element (FE) model was constructed to obtain the analytical frequencies and mode shapes. Then, the FE model of the arch bridge was tuned to minimize the difference between the analytical and experimental modal properties. Three artificial intelligence algorithms were used to calibrate uncertain parameters: the simple genetic algorithm (SGA), the simulated annealing algorithm (SAA), and the genetic annealing hybrid algorithm (GAHA). The simulation results showed that GAHA exhibited the best performance in mathematic function tests among the three methods and that the large-scale arch bridge could be efficiently calibrated using a hybrid strategy that combines SGA and SAA. To verify the admissibility of the calibration procedure, a sensitivity analysis was performed for the Young's modulus of the steel members, and the relative error for the static deformation of the bridge deck was determined. Finally, to verify the accuracy of the results, a multimodel updating method based on Bayesian statistical detection was analyzed for further validation. Through a detailed St-Id study using precise modeling, operational modal analysis (OMA), and the artificial intelligence algorithms, the authors confirmed the accuracy of the updated FE model for further structural performance prediction. **DOI:** 10.1061/(ASCE)BE.1943-5592.0001086. *© 2017 American Society of Civil Engineers.*

Author keywords: Operational modal analysis; Epistemic uncertainty; Finite-element model; Model calibration; Concrete-filled steel tubular arch bridge.

Introduction

The characterization of long-span bridges has received increasing attention in recent years not only because of the degradation of many structures and the limitations of traditional assessment approaches but also because of the increasing complexity of new bridges (Magalhães et al. 2008). Structural identification (St-Id), as proposed by Liu and Yao (Hart and Yao 1977; Liu and Yao 1978), is a systematic approach for characterizing the structural behavior of an unknown system based on the input and output test data. St-Id has been used for numerous applications, including condition assessment and maintenance management. The St-Id framework involves six basic steps: observation and conceptualization, a priori modeling, controlled experimentation, processing and interpretation of data, model calibration and parameter identification, and use of the model for simulations (Catbas et al. 2013).

In the third step of St-Id, ambient vibration tests take advantage of such natural excitation sources as traffic, wind, and microtremors and combinations of these sources. The application of ambient vibration tests is cost-effective because the measurement does not require the interruption of public traffic on bridge decks. The characteristic of ambient vibration is generally assumed as spatially distributed and broad-banded. Thus, a few operational modal analysis (OMA) methods can provide accurate estimates of natural frequencies, mode shapes, and damping ratios despite the relatively low amplitude of vibration signals. Assessments based on ambient vibration can efficiently provide accurate information concerning the actual bridge performance under working conditions. To date, several hundred applications of OMA on long-span bridges have been reported, such as those for the Golden Gate suspension bridge (Abdel-Ghaffar and Scanlan 1985), Tsing Ma Bridge (Kwong et al. 1995), Tennessee River steel arch bridge (Ren et al. 2004), Jiangyin Bridge (Ko and Ni 2005), Beichuan River bridge (Jaishi and Ren 2005; Jaishi et al. 2007), Infante D. Henrique Bridge (Magalhães et al. 2008), Svinesund Bridge (Schlune et al. 2009), Alfred Zampa Memorial Bridge (He et al. 2009), Tamar Bridge (Cross et al. 2013), and Aizhai suspension bridge (Yu and Ou 2016). It should be emphasized that Dr. Aktan's research team at Drexel University has been involved in the testing of a wide range of operating bridges using OMA as an experimental tool (Catbas et al. 2007; Grimmelsman 2006; Pan et al. 2009; Zhang et al. 2013a; Dubbs and Moon 2016).

The accurate modeling of constructed systems poses a challenge because of the significant epistemic uncertainties associated with the boundary conditions, intrinsic force distributions, nonlinear and

[1]Associate Professor, College of Civil Engineering, Hunan Provincial Key Lab on Damage Diagnosis for Engineering Structures, Hunan Univ., Changsha, Hunan 410082, P.R. China (corresponding author). E-mail: zhouyun05@gmail.com

[2]Postgraduate Student, College of Civil Engineering, Hunan Univ., Changsha, Hunan 410082, P.R. China. E-mail: jkzhang1119@126.com

[3]Professor, College of Civil Engineering, Hunan Univ., Changsha, Hunan 410082, P.R. China. E-mail: wjyi@hnu.edu.cn

[4]Postgraduate Student, College of Civil Engineering, Hunan Univ., Changsha, Hunan 410082, P.R. China. E-mail: jyzhong217@126.com

[5]Formerly, Postgraduate Student, Drexel Univ., Philadelphia, PA 19104. E-mail: qpan22@gmail.com

Note. This manuscript was submitted on April 6, 2016; approved on March 16, 2017; published online on June 9, 2017. Discussion period open until November 9, 2017; separate discussions must be submitted for individual papers. This paper is part of the ***Journal of Bridge Engineering***, © ASCE, ISSN 1084-0702.

nonstationary behaviors, and material and cross-sectional properties. Oberkampf (2005) defined two types of uncertainties: epistemic uncertainty and aleatory uncertainty. Epistemic uncertainty is caused by a lack of knowledge of the quantities or processes of the system or the environment and is also referred to as subjective uncertainty, reducible uncertainty, and model uncertainty (Ciloglu et al. 2012). Aleatory uncertainty is an inherent variation associated with the physical system or the environment and is also referred to as variability, irreducible uncertainty, stochastic uncertainty, and random uncertainty. Moon and Aktan (2006) conducted a detailed review of the impact that uncertainty has on the St-Id of constructed systems. Pan et al. (2009) discussed various sources of epistemic uncertainty and described mitigation approaches based on the St-Id of a long-span steel arch bridge. Ciloglu et al. (2012) designed a physical laboratory model to simulate four key sources of epistemic uncertainty representing the primary test variables. The results demonstrated that proven and accepted data-preprocessing techniques and modal parameter-identification algorithms can significantly bias OMA results when used in certain combinations under different structural and excitation conditions.

In the fifth step of St-Id, updating of the finite-element (FE) model entails tuning the model so that it can better reflect the measured data from the physical structure being modeled (Friswell and Mottershead 1995). Model-updating methods can basically be classified as direct methods and iterative methods based on whether the methods modify the elements of the system matrices (mass, stiffness and possibly damping matrices) directly or tune model parameters (e.g., structural geometric and material parameters) iteratively. In general, the optimum solution can be obtained by using least-squares minimization optimization methods, and methodologies based on heuristic stochastic algorithms to solve the optimization problem in St-Id have been employed in recent years; among them, simple genetic algorithms (SGAs), particle swarm optimization (PSO), ant colony optimization (ACO), artificial neural networks (ANNs), evolutionary strategy (ES), and differential evolution (DE) algorithms have gained increasing attention (Sun et al. 2013). Sun and Betti (2015) proposed a hybrid approach that is a combination of a modified artificial bee colony (MABC) algorithm and the Broyden–Fletcher–Goldfarb–Shannon (BFGS) method. Koh et al. (2003) proposed a hybrid computational strategy combining a genetic algorithm (GA) with a compatible local search operator for large-structure parameter identification. Wang (2009) developed a hybrid GA integrated with the Gauss–Newton method to identify the structural system. The classic GA and the simulated annealing algorithm (SAA) are acknowledged to offer certain advantages and have been applied to many practical problems, such as bridge maintenance and scour-depth prediction at bridge piers (Azamathulla et al. 2010; Furuta et al. 2014). The application of hybrid GA has obvious advantages over the classic GA method. When updating the high-fidelity FE model of the complex bridge structure, the high-resolution FE model is constructed on the platform of the FE packages, whereas the advanced optimization techniques, such as the GA method, can be easily implemented in numerical software such as *MATLAB* (Wan and Ren 2015). Sanayei et al. (2015) and Sipple and Sanayei (2014) developed a frequency-response function-based parameter-estimation method for model calibration of a full-scale bridge; they then developed a robust multiple-response structural parameter-estimation method for the automated FE model updating. They used *PARIS* as the automated FE model calibration code for full-scale structures, and the application programming interface (API) technique allowed real-time exchange of information between *MATLAB* and *SAP2000* during the iterative stages and the updating of model parameters in the optimization process.

In the sixth step of St-Id, the purpose of FE model updating is to fully understand the structural performance. The applications can lead to calibration of new design approaches, an understanding of deterioration mechanics, and an indication of the effectiveness of maintenance techniques, all of which can aid in decision making, especially in terms of the choice related to structural maintenance, preservation, or replacement, which involves a complicated intersection of technical, social, political, environmental, and economic considerations (Moon et al. 2010). The updated model can also be used to deduce different hypothetical scenarios in which the bridge engineer is interested, to analyze the mechanical characteristics, to establish critical regions for reliability/vulnerability analysis, and to conduct nonlinear collapse analysis; it is also useful in designing instrumentation for monitoring and for design renewal (Aktan et al. 1997).

Objective and Scope

This paper discusses the challenges that were overcome in a recent application of St-Id for a long-span arch bridge. Emphasis is placed on correlating the experimental data and the calculated data and using heuristic expertise to update the physical parameters in a complex FE model. A complete St-Id procedure, including field testing, signal processing, FE model construction, model analysis, and automatic parameter identification with the aid of an API, is presented. Field testing, including static testing under truck loads and ambient vibration testing (AVT) under natural excitations, was conducted, and the modal characteristics were extracted using two different identification techniques. A three-dimensional (3D) FE model of the bridge based on the existing drawings, which were verified through an on-site inspection, was analyzed to identify the bridge's analytical characteristics. The SGA and the genetic annealing hybrid algorithm (GAHA) were utilized to calibrate the uncertain parameters. Two methods were implemented in *MATLAB* to automatically achieve multiple-parameter identification. A parameter assessment was performed, and the admissibility of the calibrated model was verified to validate the applicability of the entire identification procedure. Finally, a multimodel identification strategy based on the Bayesian interface strategy was used to validate the identified results.

Bridge Description (Step 1)

The Laihua Bridge is a concrete-filled steel tubular arch bridge built in 2012. It is located in Laibin City, China, and crosses the Hongshui River; the main span of the bridge is 220 m long with a width of 32 m. The general layout drawings of the entire bridge are presented in Fig. 1. Each cross section of the two main arch ribs consists of four concrete-filled tubes with dimensions of ϕ 750 × 20 or ϕ 750 × 16 mm. The depth of the main arch ribs varies from 5.50 m at the footing to 3.50 m at the top with a constant width of 2.0 m. The two main arch ribs of the superstructure are connected by 10 K-type hollow steel tubes. There are 36 main suspenders, consisting of polyether sulfone steel wire ropes that are vertically attached to the main arch ribs at 7-m intervals. Below the level of the floor system, 16 concrete-filled tubes (ϕ 800, filled with C50) are supported between the arch ribs and the bridge deck. The floor system consists of a 320-mm-thick concrete slab supported by 11 longitudinal stringers (typical W16 × 77, spaced at 2.7 m). The typical sections of the floor beams have 1,780 × 16 mm webs and 50-mm cover plates. The length of the floor beams between the main wire rope suspenders is 27 m. The superstructure is supported by

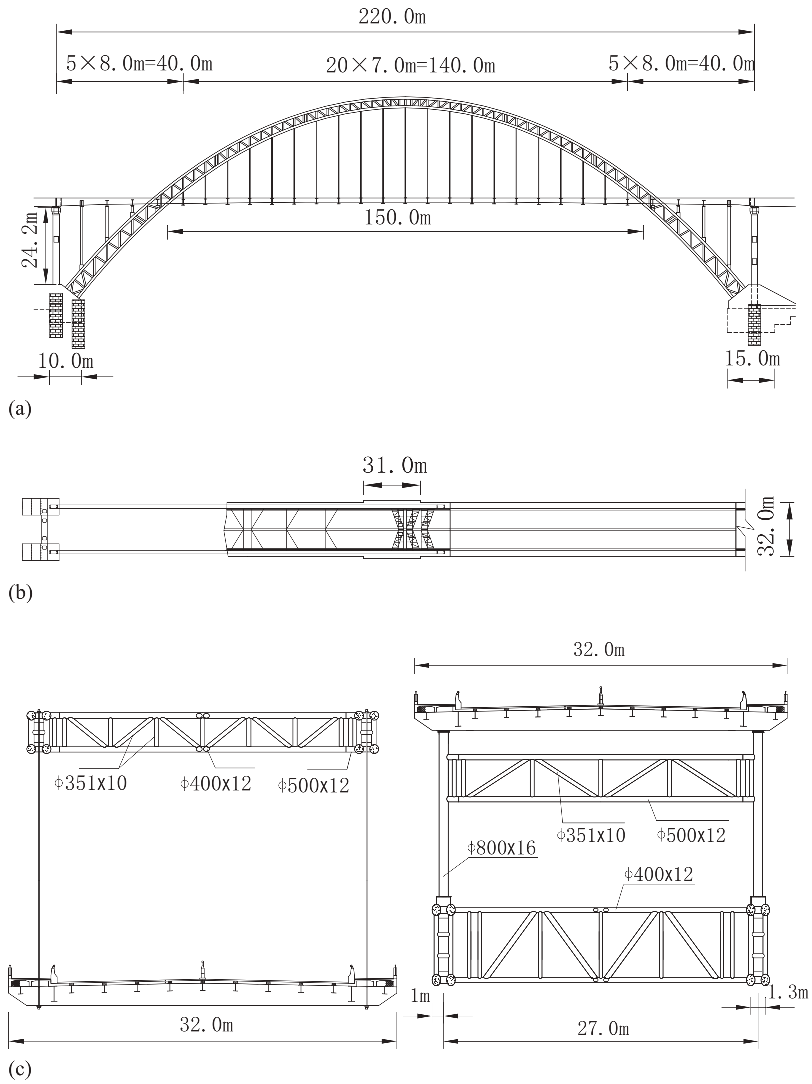

Fig. 1. Structural layout plan of Laihua Bridge: (a) elevation view; (b) plan view; (c) detailed cross-sectional drawings (Note: φ 351 × 10 means a steel tube with a diameter of 351 mm and a thickness of 10 mm)

expansion bearings, and the arches are supported on massive concrete blocks.

FE Modeling (Step 2)

Bridge Modeling

Building accurate FE models is one of the main challenges in structural analysis. Rational FE modeling must strike a balance between accuracy and calculation efficiency. To mitigate modeling uncertainty, the geometry and member details of FE models should be constructed in strict accordance with the design blueprints and field inspection. An element-level 3D FE model was constructed in *Strand7* analysis software, as shown in Fig. 2. The FE model had a total of 19,004 nodes, 22,972 beam elements, and 2,256 shell elements. The main structural members were cables, girders, floor beams, a concrete slab, and arches. The RC deck was discretized using shell elements with six degrees of freedom (DOF) at each node. Space frame elements were used to represent the deck stringers, floor beams, verticals, handrails, crash barriers, cushion caps, and arch ribs of the substructures, and the bracings were modeled using link elements to mimic the actual end connections. Both the cross girders and arch ribs of the bridge consist of variable sections, which were accurately simulated in the model. The 61 PES-7-061 Type (GB/T 18365-2001) strand cables were modeled in *Strand7* using 3D tension-only beam elements. The main arch is anchored in massive concrete blocks set on rock; fixed bearings are used for the arches, whereas expansion bearings are used for the bridge deck. Generally, there are two kinds of modeling strategies to model the concrete-filled steel tubes, unified modeling theory (Zhong 2003) and the general modeling theory, as shown in Fig. 3. After comparison of the predicted results of the modal information and static deflection, the general modeling theory, which simulates the cross section as separate sections for the steel tube and the concrete core, was chosen for the following model-updating analysis.

Sensitivity Analysis

The parameters that the modeling results were most sensitive to were identified to allow the FE model to be iteratively updated; this procedure is typically referred to as sensitivity analysis–based model calibration. In general, the parameters to which a structural model are most sensitive are the material properties and boundary

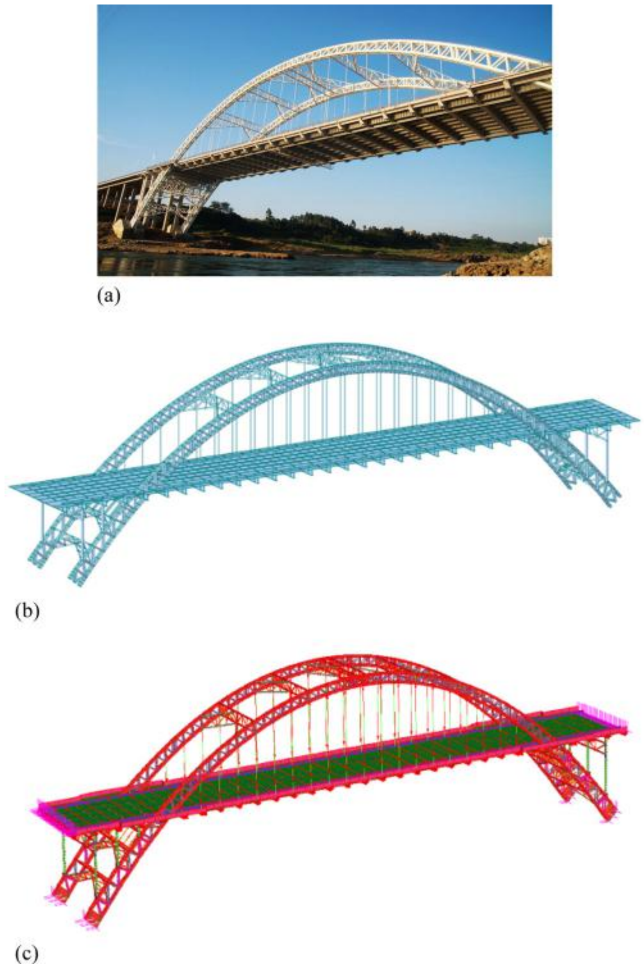

Fig. 2. (a) Laihua Bridge (image by Yun Zhou); (b) Laihua Bridge FE model in *Midas*; (c) Laihua Bridge FE model in *Strand7*

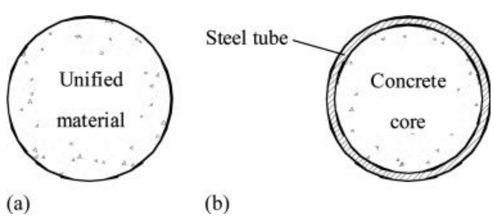

Fig. 3. Cross-sectional modeling of a concrete-filled steel tube: (a) unified theory; (b) general modeling method

conditions (Aktan et al. 1998). The critical parameters to be analyzed in this study were selected as follows:

1. The Young's moduli of the concrete arch ribs, bridge deck, pedestrian deck, verticals, and crash barriers,
2. The Young's moduli of the steel arch ribs and stay cables, and
3. The vertical stiffness boundary conditions at the ends of the bridge deck.

Generally, a sensitivity analysis is based on an FE model representation of a physical system and attempts to assess the sensitivity of the objective function to variations in uncertain parameters. This study used two types of objective functions, one concerning deflections under static loading conditions and one concerning modal frequencies and mode shapes (Jaishi et al. 2007), as shown in Eqs. (1) and (2), respectively.

$$F(x) = \sum_{i=1}^{10} |d_{ai} - d_{ei}| \tag{1}$$

where d_{ai} = deflections predicted by the FE model; d_{ei} = experimentally measured values; x = the uncertain parameter chosen for the sensitivity analysis; and i = the ith measurement point in the full static test.

$$F(x) = \sum_{i=1}^{m} \left(\frac{f_{ai} - f_{ei}}{f_{ei}} \right)^2 + \sum_{i=1}^{m} \frac{\left(1 - \sqrt{\text{MAC}_i}\right)^2}{\text{MAC}_i} \tag{2}$$

where f_{ai} = frequencies predicted by the FE model; f_{ei} = frequencies calculated by the SSI method; x = the uncertain parameter chosen for the analysis; i = the ith considered mode; and m is the number of mode shapes considered. Modal assurance criteria (MACs), as shown in Eq. (3), were used to evaluate the correlations between mode shapes.

$$MAC_i = \frac{\left(\Phi_{ai}^T \Phi_{ei}\right)^2}{\left(\Phi_{ai}^T \Phi_{ai}\right)\left(\Phi_{ei}^T \Phi_{ei}\right)} \tag{3}$$

where Φ_{ai} = mode shape predicted by the FE model; Φ_{ei} = mode shape identified by the SSI method; and i = the ith considered mode.

A sensitivity analysis with respect to the initial estimates of the parameters was performed for nine influential parameters by curve fitting, as shown in Fig. 4. The sensitivity analyses shown in Figs. 4(a, c, and e) relate to static deflection, whereas the analyses shown in Figs. 4(b, d, and f) relate to the modal parameters. The most sensitive parameters identified using the static loading data and the modal data were almost the same, and the two different objective functions showed similar trends with respect to variations in the boundary conditions.

Dynamic and Static Tests (Step 3)

Ambient Vibration Testing

Prior to the official opening of the bridge in June 2013, full-scale AVT was conducted on the Laihua Bridge, and dense instrumentation layouts were established on the bridge deck and the arch ribs in the vertical and lateral directions. An LMS International (Leuven, Belgium) Cada-X data-acquisition system with eight channels was used to simultaneously record the ambient vibration signals. KD12000L ultralow-frequency accelerometers (20 V/g) were installed on the bridge deck and arch ribs; of these accelerometers, six were moved among various measurement points, and the other two were used to establish fixed reference points (Fig. 5). The reference points were selected according to the preliminary information obtained from a modal analysis of the FE model to avoid placing the measurement instruments on modal node points. A sampling frequency of 512 Hz was chosen, and each data set was collected for a duration of 15 minutes. The typical signals in the vertical and transverse directions are shown in Fig. 6.

Full Static Loading Tests

Diagnostic load testing, such as truck load testing, is an independent experimental tool in St-Id and can be regarded as complementary to global modal testing. When properly conducted, static loading tests provide excellent verification of the AVT results and serve as a valuable tool for exploring the localized characteristics of a bridge. Static loading tests of the Laihua Bridge were conducted using a level gauge on the bridge deck to measure its deformation and a general total station to measure the deflections of the arch ribs. Full static loading tests

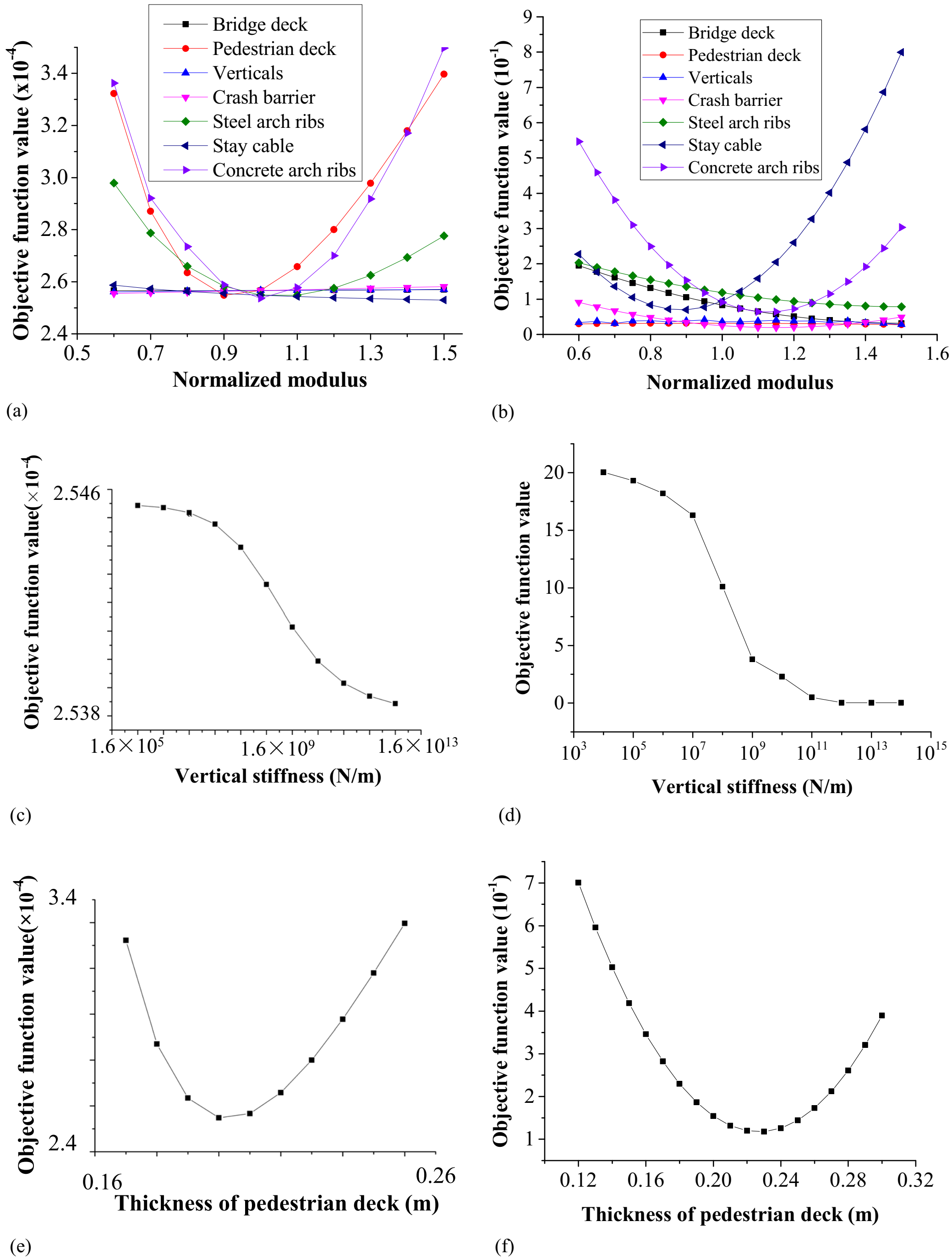

Fig. 4. Variations in the value of the objective function: (a) versus Young's modulus using the static test data; (b) versus Young's modulus using the modal test data; (c) versus boundary conditions using the static test data; (d) versus boundary conditions using the modal test data; (e) versus thickness of the pedestrian deck using the static test data; (f) versus thickness of the pedestrian deck using the modal test data

were performed for 20 different cases in different configurations. Trucks with known wheel loads were positioned at 1/4 of the bridge span, and the corresponding displacements were measured.

Dynamic Signal Processing (Step 4)

Dynamic Signal Analysis

In OMA, the structure is excited by unknown input forces (such as wind, traffic, earthquakes, and waves), and only output data are acquired. A data quality check should be conducted first to ensure a reliable OMA. The quality of the data was evaluated by visually inspecting both the time and frequency domains using the fast Fourier transform (FFT) technique. Spurious responses in the time history of each channel were removed to preserve the maximum acceptable response data.

In many previous applications of dynamic signal analysis, a number of missing modes or sporadic modes have appeared or disappeared depending on the various preprocessing and postprocessing techniques. The reasons for such modes and the reliability of intermittent modes are fundamental questions that continue to challenge OMA. The uncertainty introduced by the presence or absence of such modes is difficult

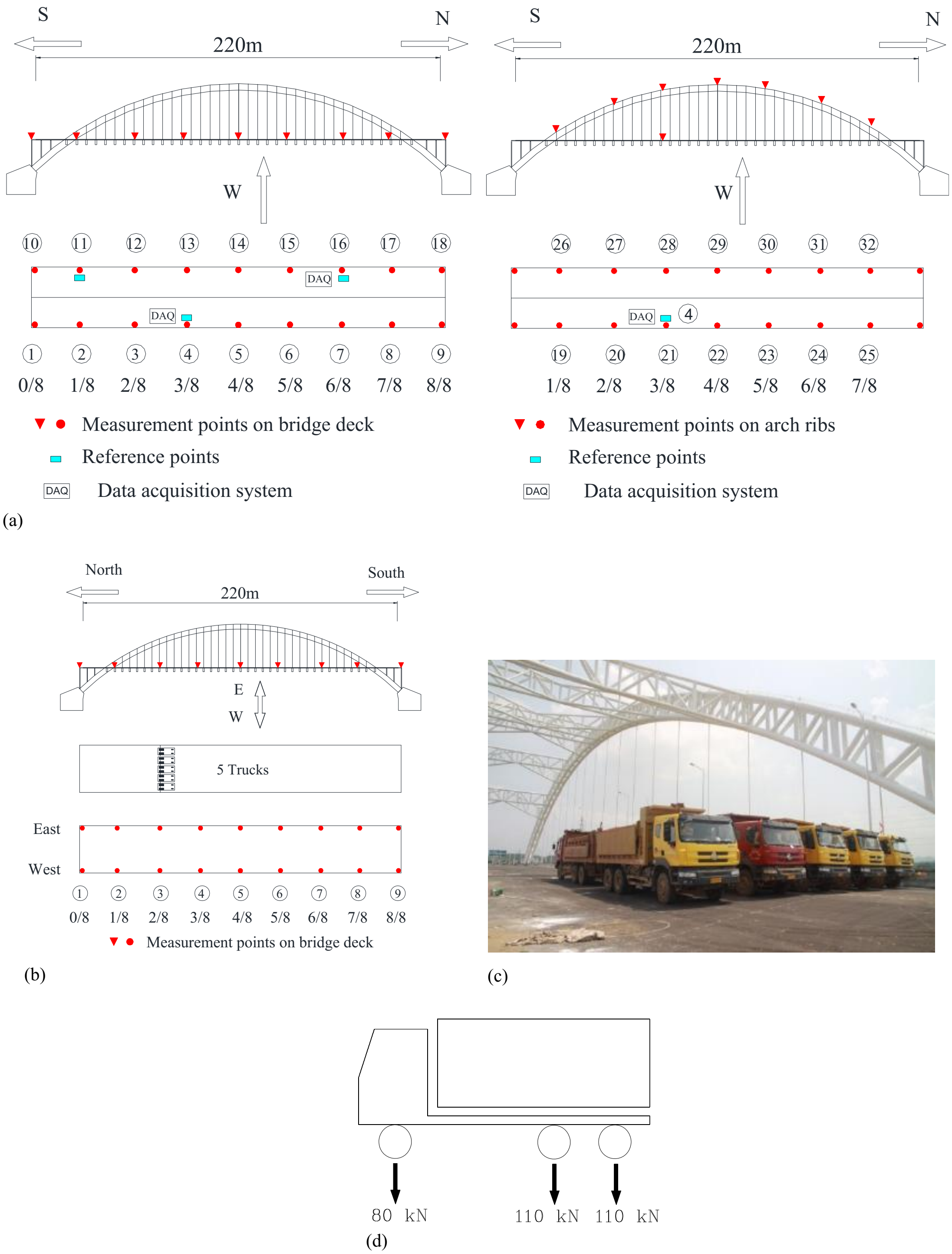

Fig. 5. (a) Instrumentation layout; (b) static truck loading tests at 1/4 of the span; (c) case with 10 trucks at 1/4 of the span (image by Yun Zhou); (d) detailed truck load

to address using probability theory and represents a key source of epistemic uncertainty. To eliminate the influence of epistemic uncertainty, the results of the random decrement (RD) technique in combination with the complex mode indicator function (CMIF) were compared with the results of the SSI technique in the following analysis.

Operational Modal Analysis

The basis of the CMIF method is the singular value decomposition (SVD) of a multiple-reference function matrix, whereas the SSI method is based on the discrete state-space formulation that represents the dynamic system behavior. Previous research on these two identification approaches includes the studies performed by Shih et al. (1988), Phillips et al. (1998), and Peeters and DeRoeck (1998). In this study, the complex mode indicator plot obtained using the CMIF approach and the stabilization diagram obtained using the SSI method clearly indicate consistency in the modal frequency estimations (Fig. 7). For most long-span bridges, the frequency range of interest lies between 0 and 10 Hz, which contains most of the relevant modal characteristics. The identified natural

J. Bridge Eng., 2017, 22(8): 04017049

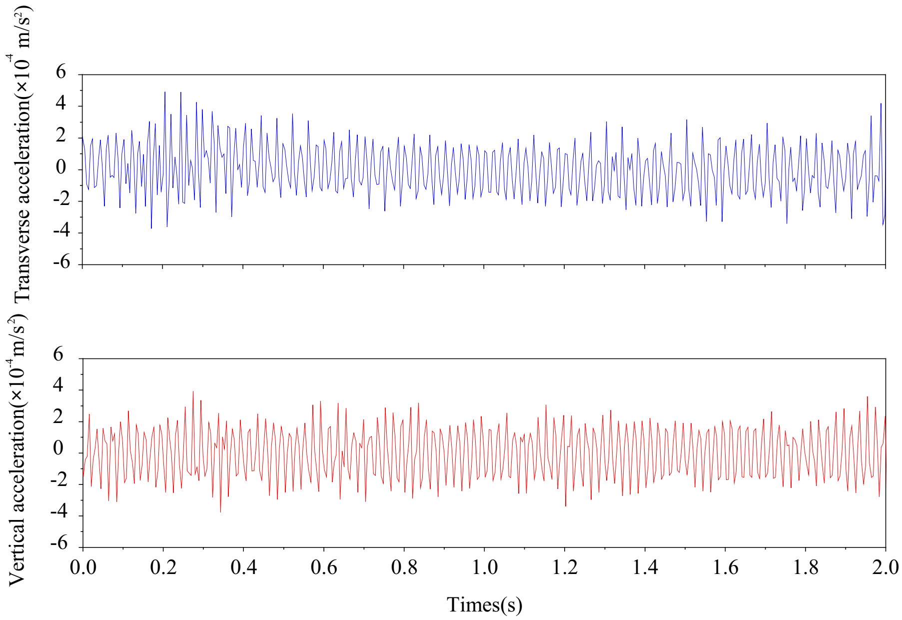

Fig. 6. Typical vertical and lateral vibration signals on the bridge deck

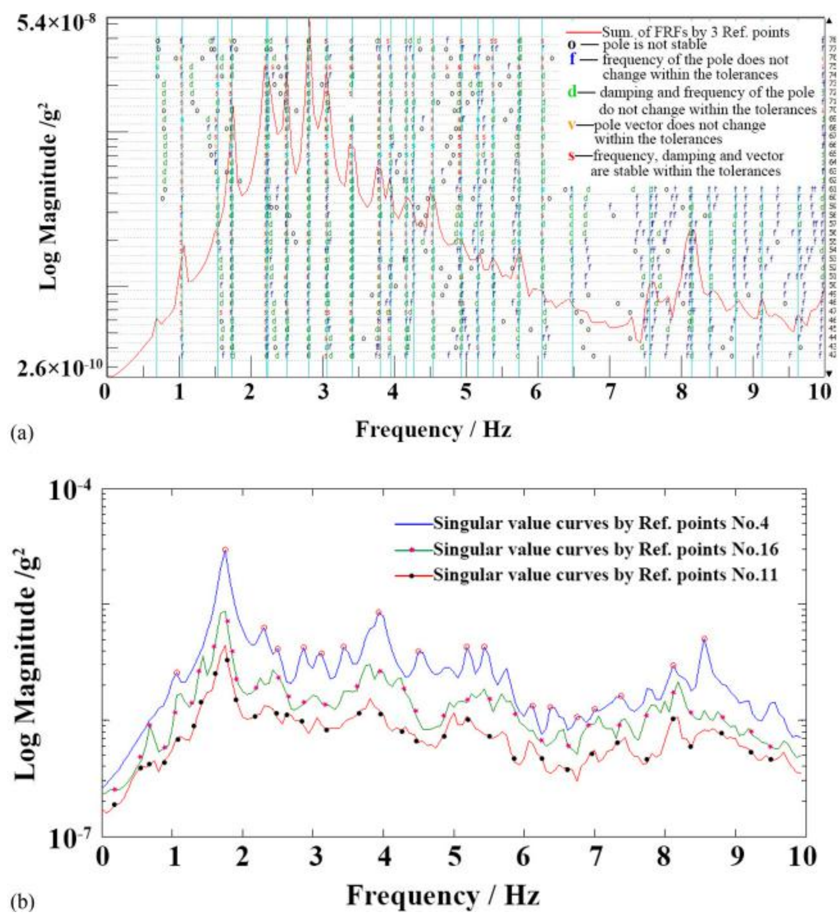

Fig. 7. Vertical vibration data: (a) stabilization diagram; (b) CMIF plot

Table 1. Comparison of Experimental and Analytical Frequencies

Mode number	Experimental frequencies (Hz)		Analytical frequencies (Hz)			
	SSI	RD + CMIF	*Strand7*	Error (%)	*Midas*	Error (%)
1	0.694	0.695	0.708	2.09	0.570	17.80
2	1.040	1.064	1.082	4.09	1.049	0.86
3	1.531	1.550	1.394	8.95	1.380	9.86
4	1.730	1.751	1.763	1.90	1.739	0.52
5	2.243	2.314	2.285	1.89	2.020	9.94
6	2.503	2.509	2.501	0.08	2.490	0.52
7	2.808	2.875	2.829	0.73	2.770	1.35
8	3.406	3.438	3.461	1.60	3.338	1.99
9	3.949	3.937	3.815	3.39	3.796	3.87
10	4.536	4.502	4.618	1.80	4.014	11.51

Note: Error (%) $= \left(f_{\text{analysis}} - f_{\text{experiment\_SSI}}\right)/f_{\text{experiment\_SSI}} \times 100\%$.

frequencies and mode shapes of the first 10 vibration modes are summarized in Table 1 and Fig. 8. The identified damping ratios are very low, which is consistent with the results of previous St-Id studies of long-span arch bridges (Ren et al. 2004).

Mode Coupling

In this study, ambient vibration signals were measured in the vertical and transverse directions. Because of the number of sensors and the different signal-to-noise ratios typically associated with different response directions, it is common to postprocess data sets to obtain two-dimensional (2D) mode shapes in each direction separately. However, strong spatial coupling was evident in the vibrations of the bridge deck and arch ribs, indicating that the 2D postprocessing approach might be not sufficient for revealing the actual behavior of the structure in multiple directions. Fig. 9 shows the spatial mode coupling at 2.503 Hz, and Table 2 specifies several of the coupling modes of the bridge deck and arch ribs.

It has to be indicated that the modes of the bridge deck may be a better choice over the modes of the arch rib in the following model calibration procedure for two reasons: (1) the number of modes of the arch ribs that could be excited was much less than that of the bridge deck because the stiffness of the arch ribs was much larger than that of the bridge deck, therefore making it more difficult to excite the vibration modes of the arch ribs; and (2) the identifiability of the arch rib vibration modes was much lower than that of the bridge deck, as can be judged from the fact that the curves of some measured vibration modes of the arch ribs were not smooth and symmetric as would normally be expected.

Optimization Methods and Model Calibration (Step 5)

Artificial Intelligence Algorithms

The SGA is a bionic random algorithm that mimics the biological process of natural genetics and natural selection (Goldberg 1989). It is performed using a number of individuals, and adaptive solutions are propagated from one generation to the next until the termination criterion is satisfied. Computationally simple and powerful, SGAs are practical methods for searching for global optima without previous information (Krishnamoorthy et al. 2002; Castillo et al. 2007; Cheng and Yu 2013). The SAA is an iterative method in which an initial solution is gradually improved by making local changes with a probability that depends on temperature. This method was first introduced by Kirkpatrick et al. (1983), and it has been widely applied to large-scale combinatorial problems (Mantawy et al. 1998; Aydin and Fogarty 2002). Recently, recognition of the complementary strengths of SGA and SAA has led to the development of a hybrid method to achieve a more efficient search for complex combinatorial problems (Blum and Roli 2008). In the proposed GAHA, the optimization operators, the fitness evaluation function, and SAA integration strategies are designed to improve the convergence, as illustrated in Fig. 10. In the early stage, the GAHA performs a parallel search with high efficiency to avoid premature convergence, and in the later stages, a fine-tuned search can be achieved using the SAA. GAHA has been applied to many complicated engineering problems, such as global function optimization and the discrete time–cost trade-off problem (Chen et al. 2005; Sonmez and Bettemir 2012).

Global Calibration

In this study, model calibration through nonlinear optimization was coded in *MATLAB* and applied with the help of an API. The API technique enables users to create and calibrate model parameters in *Strand7* through coding in *MATLAB*; another advantage of the API is its ability to link to *MATLAB* toolboxes.

In SAA, it requires a relatively small number of parameters, including the cooling ratio (α), the maximum number of generations (MAXGEN), and the initial and final temperatures T_0 and T_f, respectively. As each generation develops, the value of the objective function for the current state is denoted by E_i, and the value after the application of a perturbation mechanism is denoted by E_j. The perturbation will be accepted with a probability p given by

$$p = \exp\frac{(E_j - E_i)}{b \times \alpha^T} \tag{4}$$

where b = a constant; p is to be compared with a randomly generated number between 0 and 1; and T = the temperature that slowly decreases from one generation to the next. If $p > \text{rand}(1)$, then the perturbation is accepted.

To verify the effectiveness of the proposed GAHA algorithm in solving optimization problems, three classic mathematic benchmark functions with 20 unknown variables were tested: Ackley function, Griewank function, and Rosenbrock function (Sun and Betti 2015; Zhu and Kwong 2010). In SGA and GAHA, the SGA parameters were applied based on an initial population consisting of 40 individuals with 10,000 generations and a generation gap of 0.9. In SSA and GAHA, the SAA parameters were set as $T_0 = 90$, $T_f = -10$, $\alpha = 0.95$, and MAXGEN = 10,000. The stopping criteria for SGA, SAA, and GAHA were when the objective function reached

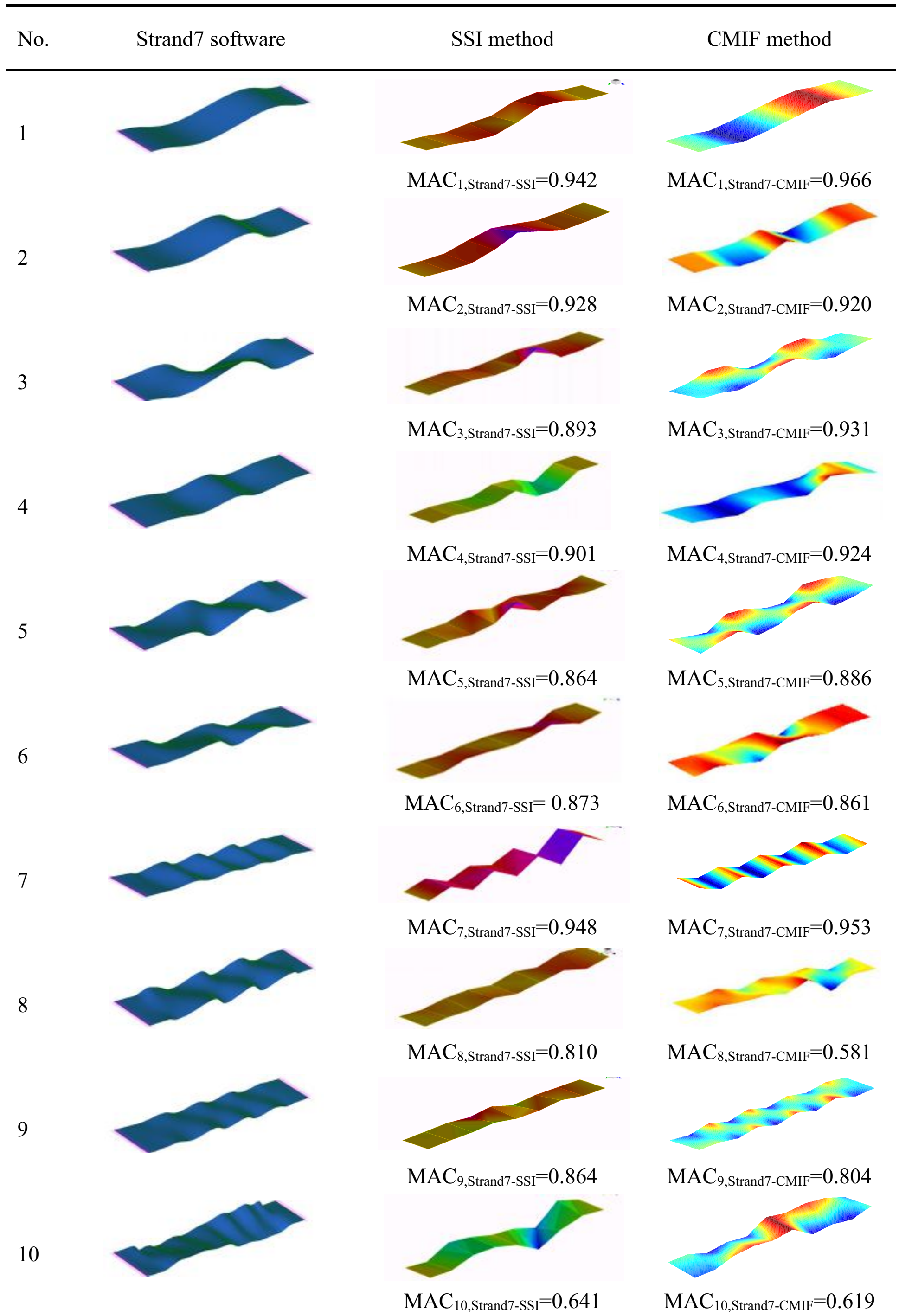

Fig. 8. Calculated and experimental mode shapes

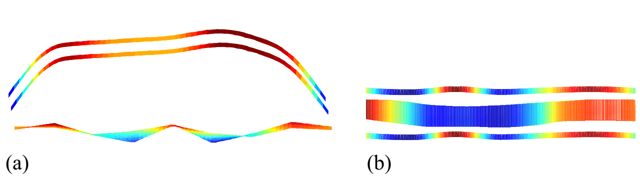

Fig. 9. Spatial mode coupling at 2.503 Hz: (a) elevation view of the vertical modes; (b) plan view of the transverse modes

the maximum number of generations. The convergence lines of the three benchmark functions are shown in Fig. 11. Although three algorithms resulted in different convergence rates and solution accuracies in different functions, it can still be seen that the proposed GAHA algorithm had a better performance than the SGA and SAA. The SAA converged on an infeasible design because it began from a random point and then worked its way toward the minimum, meaning that a local minimum is more likely to be reached. Considering the convergence rate of the different algorithms, only the SGA and GAHA were utilized in the following analysis.

Table 2. Spatial Coupling of the Bridge Deck and Arch Rib Vibrations in Certain Modes

Mode sequence	Vertical vibration of the bridge deck (Hz)	Transverse vibration of the bridge deck (Hz)	Vertical vibration of the arch ribs (Hz)	Transverse vibration of the arch ribs (Hz)
Second	1.040	—	1.064	—
Third	1.531	—	1.503	1.506
Fourth	1.730	—	1.751	—
Sixth	2.503	2.503	2.503	2.508
Seventh	2.808	—	2.876	—

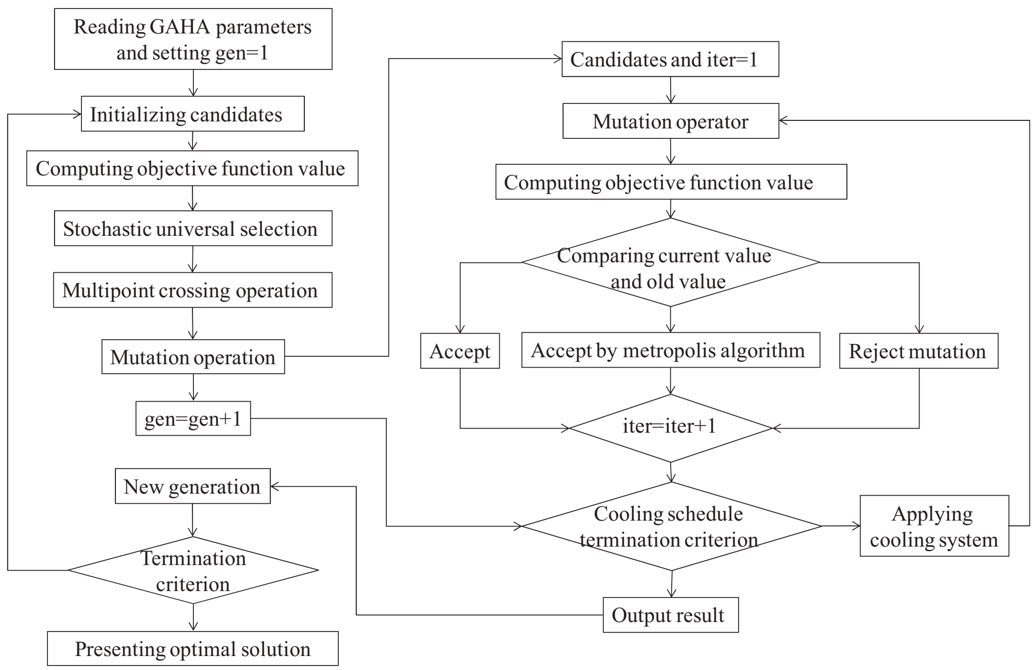

Fig. 10. Flowchart of GAHA

For the parameter identification of the bridge, it was assumed that the field test data were reliable, and an absolute percentage error for the modal information as illustrated in Eq. (2) was used. As presented earlier, the sensitivity analysis revealed five parameters with significant relative importance. Among these parameters, the thickness of the pedestrian deck, which is regarded as a certain parameter in the real structure, could be selected to validate the applicability of the optimization methods. The SGA and GAHA were used to search for the global minimum value of the objective function. The selected parameters were estimated in each generation, and the optimization procedure was terminated when a predefined number of generations was reached. In this study, the SGA and GAHA were applied based on an initial population consisting of 50 individuals with 50 generations and a generation gap of 0.9. The GAHA parameters were defined empirically as follows: $T_0 = 90$, $T_f = -10$, MAXGEN = 100, and $\alpha = 0.98$.

Identified Results

The sensitivity analysis revealed that the modal data and static load deflections were significantly affected by the vertical stiffness at the ends of the bridge deck. In the initial FE model, the boundary condition was represented by separate spring-damping elements constrained in the vertical direction. Rigid links were used in the transverse and longitudinal directions to simulate the interfaces of adjacent bridge deck sections. After calibration, the bearings in the vertical direction were assumed to be pinned, which agrees well with the field test results. The second step of calibration was to update the uncertain parameters in the initial model to align with the modal frequencies and mode shapes identified via OMA. The evolution processes of SGA and GAHA are shown in Fig. 12. The ratios of the optimal value of each parameter after calibration relative to the initial design value are presented in Fig. 13. Among the updated models obtained in this way, the model calibrated using the GAHA method showed much better agreement with the OMA results. The changes in the selected parameters to be updated are listed in Table 3, and the final analytical frequencies after calibration are given in Table 4. One important concern in model calibration is to check the physical meanings of the uncertain parameters against typical observations in practice. The updated values of the Young's modulus of the concrete arch ribs and the bridge deck increased, whereas the other values slightly decreased, which is consistent with the possibility that the concrete in the steel tubes may be confined and the fact that the dynamic modulus of concrete is larger than its static modulus.

Admissibility Check

A model admissibility check, which consisted of two steps, was conducted as a validation procedure to evaluate whether the calibrated model was suitable for simulating the real structure. The reliability of the changes to the initial FE model and the agreement between the

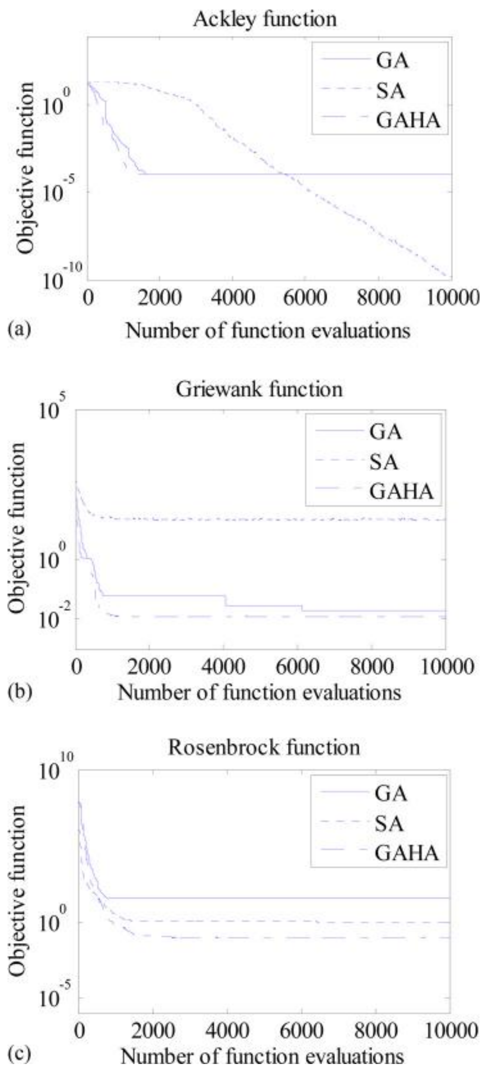

Fig. 11. Convergence lines of three benchmark mathematic functions of 20 dimensions: (a) Ackley function; (b) Griewank function; (c) Rosenbrock function

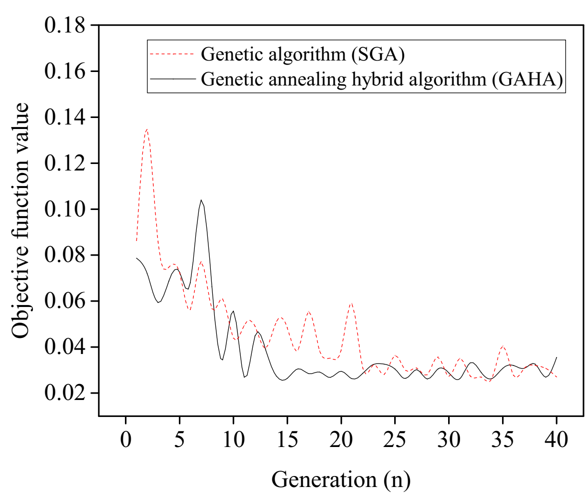

Fig. 12. Evolution processes of SGA and GAHA

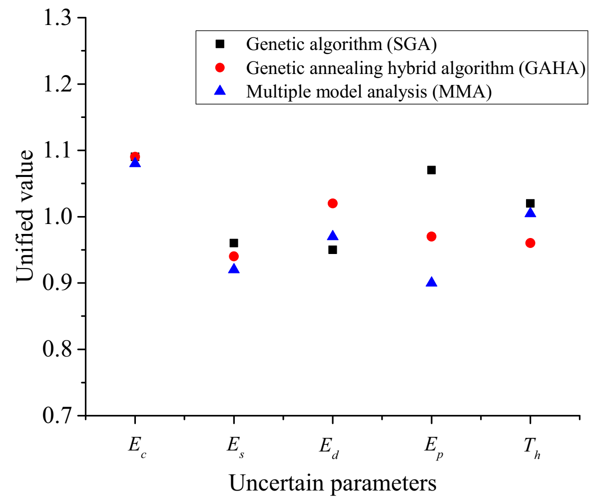

Fig. 13. Results of uncertain-parameter identification using the three optimization algorithms and multimodel method (Note: E_c, E_s, E_b, E_p, and D_p denote the moduli of the concrete arch ribs, the steel arch ribs, the bridge deck, and the pedestrian deck and the thickness of the pedestrian deck, respectively)

Table 3. Parameters of the FE Model before and after Calibration Using GAHA

Parameter updated	Initial value	Updated value	Change (%)
Modulus of concrete arch ribs (MPa)	3.74×10^4	4.09×10^4	9.36
Modulus of steel arch ribs (MPa)	2.27×10^5	2.13×10^5	–6.17
Modulus of bridge deck (MPa)	6.86×10^4	7.02×10^4	2.33
Modulus of pedestrian deck (MPa)	4.64×10^4	4.51×10^4	–2.80
Thickness of pedestrian deck (m)	0.2	0.19	–5.00

numerical and experimental data were checked, but this was not sufficient for a physically meaningful updated model. In this paper, the Young's modulus of steel was generally regarded as a near-deterministic parameter. After global correlation, the error index was minimized when the Young's modulus was set to its nominal value. After calibration, the changes to all uncertain parameters were found to be less than 10%, which is acceptable considering the epistemic uncertainties. Moreover, as a deterministic parameter in the real structure, the thickness of the pedestrian deck remained close to its nominal value after calibration with two algorithms. Afterward, a sensitivity analysis considering the modulus of the steel girders, which was known to be nearly deterministic, was performed. Unlike the initial FE model, the objective function values of the calibrated models were minimized when the Young's modulus of the steel girders was set to its nominal value, as shown in Fig. 14(a). Moreover, the deflections of the bridge deck were also checked, and the relative error at every measurement point in the static loading tests was determined. Generally, the maximum relative error between the measured and simulated deflections was reduced from 7.35 to 3.22% [Fig. 14(b)].

Double Validation by the Multimodel Approach

Because of the presence of two different kinds of uncertainties, there are challenges associated with errors and parameter compensation inherent to inverse tasks. The multimodel approach is developed

Table 4. Analytically Identified Natural Frequencies after Model Updating

		Frequencies after model calibration				
Mode number	SSI frequency (Hz)	SGA (Hz)	Error (%)	GAHA (Hz)	Error (%)	MAC
1	0.694	0.707	1.91	0.706	1.78	0.977
2	1.040	1.080	3.89	1.081	3.90	0.946
3	1.531	1.422	7.09	1.424	7.00	0.908
4	1.730	1.760	1.71	1.762	1.87	0.881
5	2.243	2.278	1.54	2.284	1.83	0.899
6	2.503	2.490	0.51	2.485	0.72	0.870
7	2.808	2.819	0.38	2.816	0.28	0.895
8	3.406	3.455	1.45	3.461	1.61	0.867
9	3.949	3.808	3.58	3.816	3.38	0.774
10	4.536	4.610	1.64	4.622	1.89	0.793

Note: $\mathrm{Error}(\%) = |f_{\mathrm{analysis}} - f_{\mathrm{experiment}}|/f_{\mathrm{experiment}} \times 100\%$.

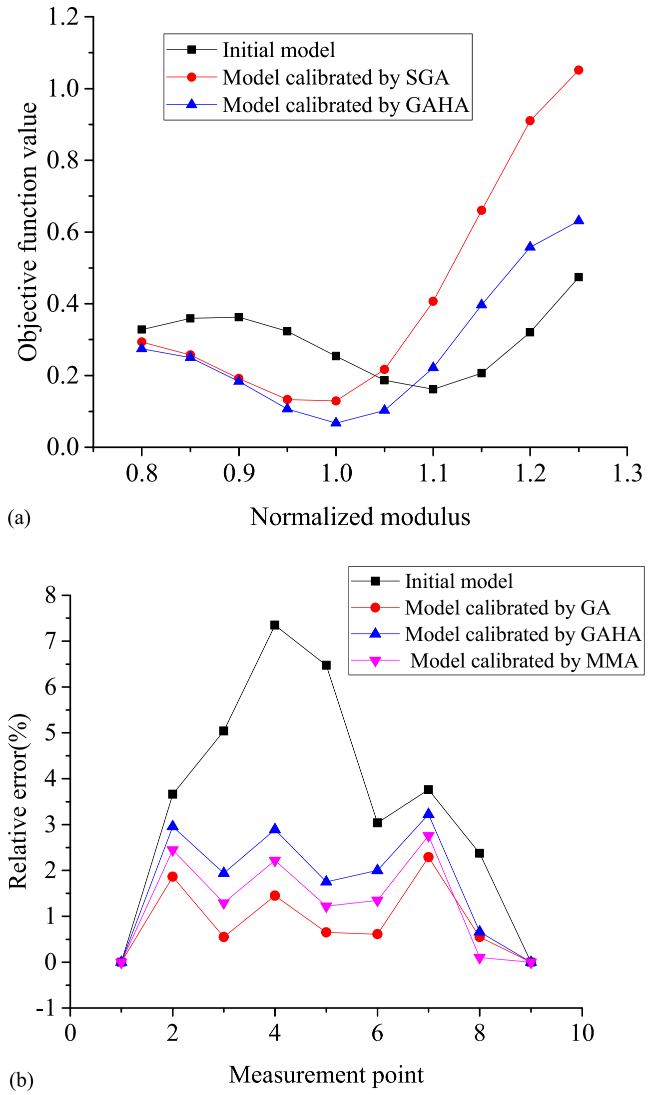

Fig. 14. (a) Sensitivities of the initial model and the models calibrated using SGA and GAHA with respect to the Young's modulus of the steel girders; (b) relative errors between the measured and simulated deflections when the truck was loaded at 1/4 point

(Raphael and Smith 1998) after all sources of uncertainties have been explicitly taken into account. The difference of the deterministic model-updating approach lies in its search for multiple candidate models that explain the measurements taken from a structure. By studying a number of candidate models consisting of variables representing key uncertainties, all possible structural parameter sets and various uncertainties are investigated. Thus, structural prediction using the multimodel method is more realistic for supporting a risk-based decision-making process. Model fragments partially describe components and physical phenomena, and a complete model is created by combining fragments that are compatible (Smith and Saitta 2008). To model the behavior of structures, the fragments represent support conditions, material properties, geometric properties, nodes, elements, and loads. The multimodel St-Id method uses multiple models to predict the measured results; the key step is to select the correct models from the model clusters. A group of FE models that matches the real structural response can be incorporated to identify correlations and clusters of the candidate model populations that can be employed in the current framework for more efficient St-Id. Over the past 15 years, the research team led by Professor Smith has conducted a series of preliminary studies of multimodel system identification (Raphael and Smith 2003; Robert-Nicoud et al. 2005).

Bayesian inference is an especially useful tool to address this problem by combining the prior knowledge of the structure with the observed vibration data into a statistical framework. The success of the Bayesian inference for FE model updating relies on the effective application of proper stochastic simulation methods (Ching et al. 2006; Cheung and Beck 2009). Bayesian model-updating techniques make it possible to identify a set of plausible models with probabilistic distributions and to characterize the modeling uncertainties of a structural system. Recently, Markov chain Monte Carlo (MCMC) sampling has been used to quantify parameter uncertainties in model updating for the reliable assessment of a footbridge and a 21-story concrete building (Sun et al. 2017; Behmanesh and Moaveni 2015).

In this study, Bayesian model updating was utilized via MCMC sampling and weighing based on Bayes' statistic theorem, and the multimodel method was used to validate the accuracy of the results of the single-model updating method. Based on the Bayesian statistical detection and error analysis, the multimodel updating builds random model clusters using random sampling. Through the analysis of measured data and the FE model analysis results, the posterior probability can be calculated from the prior probability and likelihood function (Zhang et al. 2013b) based on Eq. (5), as follows:

$$p\left[M_i(\theta)/D\right] = \frac{p\left[D/M_i(\theta)\right]p\left[M_i(\theta)\right]}{\sum_{i=1}^{n} p\left[D/M_i(\theta)\right]p\left[M_i(\theta)\right]} \tag{5}$$

Table 5. Prior and Posterior Distribution of the Model Fragments

Model fragment	Initial value	Prior distribution	Maximum posterior estimate	Change (%)
E_c	3.74×10^4 MPa	N(1.0,0.2)	4.06×10^4 MPa	8.56
E_s	2.27×10^5 MPa	N(1.0,0.2)	2.08×10^5 MPa	–8.37
E_d	6.86×10^4 MPa	N(1.0,0.1)	6.68×10^4 MPa	–2.62
E_p	4.64×10^4 MPa	N(1.0,0.2)	4.17×10^4 MPa	–10.13
T_h	0.20 m	N(1.0,0.1)	0.20 m	0

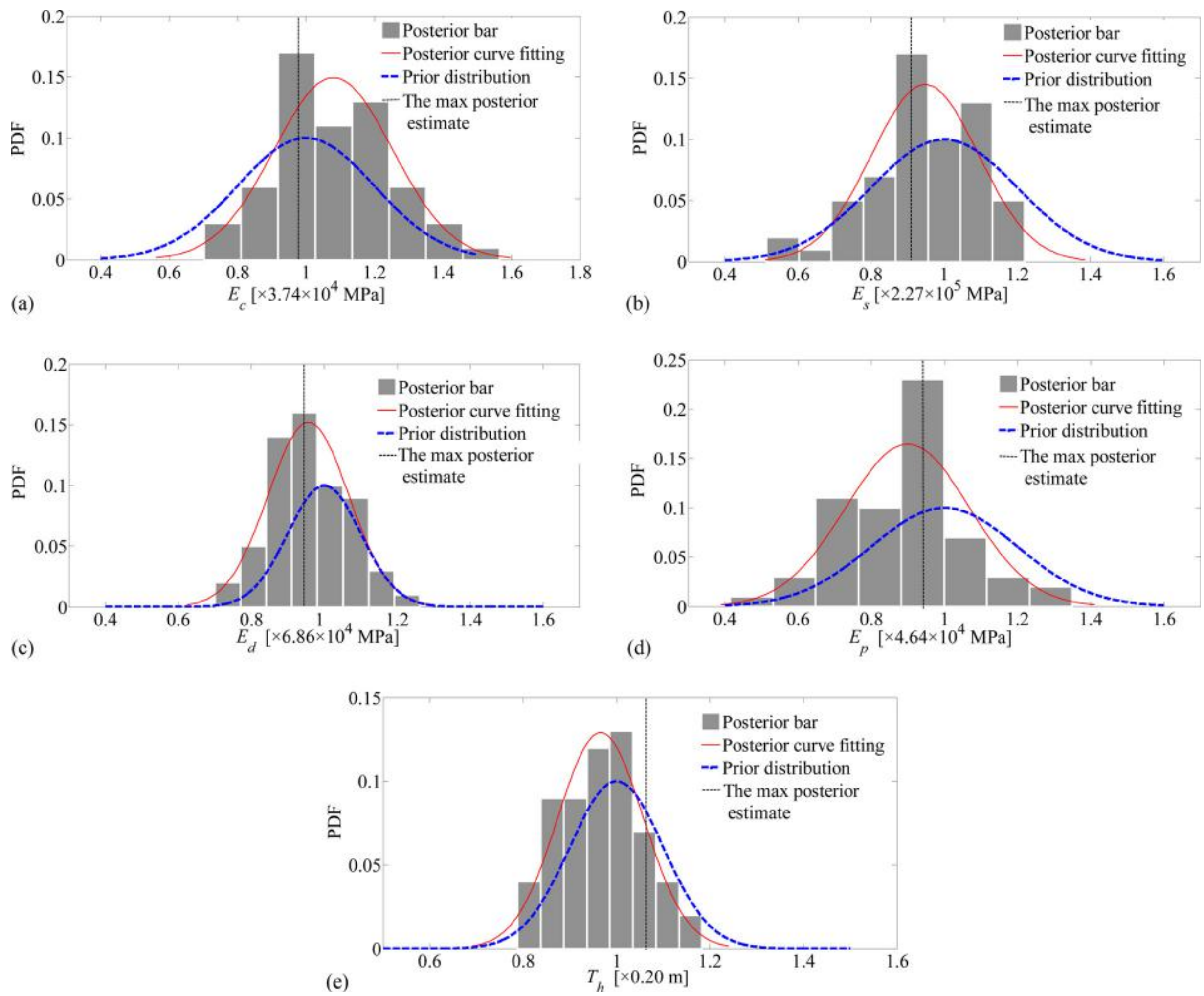

Fig. 15. Identified physical parameters of model fragments in the Laihua Bridge model: (a) E_c denotes the modulus of the concrete arch ribs; (b) E_s denotes the modulus of the steel arch ribs; (c) E_b denotes the modulus of the bridge deck; (d) E_p denotes the modulus of the pedestrian deck; (e) T_h denotes the thickness of the pedestrian deck

where θ = vector of uncertainty parameters of the structure; and $p[M_i(\theta)]$ = initial (prior) probability of each model when the uncertain parameter has a prior distribution based on engineering and modeling judgment. Because each model fragment is sampled individually, the prior probability of each model equals the product of multiplying each model fragment. $p\left[D/M_i(\theta)\right]$ presents the likelihood function, which can be presented as $p(x|\theta) = \prod_{s=1}^{N_m} p(\widehat{f}_s|\theta)p\left(\widehat{\phi}\,|\theta\right)$ (Zhou 2008), in which $\widehat{f}_s$ and $\widehat{\phi}_s$ are measured frequencies and mode shapes. $\sum_{i=1}^{n} p\left[D/M_i(\theta)\right]p[M_i(\theta)]$ is a normalizing constant called the Bayesian factor, which can be regarded as the marginal probability distribution. Using the Metropolis–Hasting (M-H) algorithm, the method begins by selecting a starting point θ_i. A sample is drawn from the proposal function q(x,y). The proposal function is assumed to be the form of a normal distribution. The acceptance ratio can be calculated by Eq. (6), as follows:

$$\alpha(x_t, y_{t+1}) = \frac{\pi(y_{t+1})q(x_t, y_{t+1})}{\pi(x_t)q(y_{t+1}, x_t)} \tag{6}$$

The proposed sample is accepted with a probability of min (1.0, α) (Dubbs 2012).

In this study, *MATLAB* software was used for MCMC-approach coding. Based on prior experience, the prior distribution is shown in Table 5, where E_c, E_s, E_d, E_p, and T_h represent previously defined uncertainty parameters. The Markov chain consisting of 1,000 samples was generated to present the likelihood function. The measured 10 modes were used for the MCMC calculation. The posterior distribution of the model fragment can be estimated using Fig. 15, in which the histogram denotes the probability-density functions (PDFs) obtained from MCMC sampling, the solid red line denotes the PDFs through curve fitting using the normal distribution, the dashed curve-fitting line denotes the maximum a posteriori estimate, and the solid curve-fitting line presents the prior distribution. The parameter-identification results are presented in Table 5, which shows that they are close to the single-model updating results.

Conclusions

This paper presents the results of a complete St-Id study on a long-span concrete-filled steel tubular bridge, with a focus on mitigating various uncertainty factors in the initial model. By systematically performing full-scale AVT and static loading tests, the physical properties in the FE model were updated in detail through calibration using two different optimization methods. Based on the research results, the main conclusions are as follows:

1. After an initial 3D FE model was established, a careful investigation of the critical bridge members and the interaction of the bridge deck and arch ribs was performed to mitigate modeling uncertainties. A sensitivity analysis considering the results of both static and modal tests is a powerful means of identifying highly uncertain parameters. Given that epistemic uncertainty governs the behavior of long-span bridges in St-Id, the application of an analytical process consisting of precise 3D FE modeling and field tests is helpful for the reliable St-Id of complex real structures.
2. Because of a number of missing modes or spurious modes that can appear or disappear depending on the preprocessing and postprocessing techniques used, various OMA techniques were used to reduce the measurement errors induced by signal processing. The results of two independently applied methods (RD + CMIF and SSI) showed excellent agreement, confirming the overall applicability of the AVT and OMA procedure.
3. After model calibration using two different artificial intelligence algorithms (SGA and GAHA), the optimal values of the parameters were identified to avoid the parameters tapping into local minima. The high-resolution bridge FE model was constructed in *Strand7*, which interfaced with three optimization techniques in *MATLAB* to update the multiple bridge parameters automatically. Among the updated models, GAHA showed the best agreement with the AVT results and the best performance in a modal admissibility check. After calibration, the average error between the analytical (GAHA) and experimental frequencies was reduced to 2.42%, and the maximum relative error on the static load deflections was reduced from 7.35 to 3.22%.
4. The multimodel St-Id method was used to evaluate the physical parameters of the bridge to again validate the accuracy of the single-model updating method. The Bayesian inference strategy was introduced along with the Monte Carlo sampling method to generate 1,000 FE models. The posterior distribution was calculated, and the inference results were close to the updated physical parameters generated by the single-model St-Id method.

Acknowledgments

The authors are grateful for the support provided for this research by the National Key Research and Development Program of China (Grants 2016YFC0701400, 2016YFE0127900, and 2016YFC0701308), the National Natural Science Foundation of China (NSFC) (Grant 51208190), and the Research Fund for the Doctoral Program of Higher Education of China (Grant 20120161120028).

References

Abdel-Ghaffar, A. M., and Scanlan, R. H. (1985). "Ambient vibration studies of Golden Gate Bridge. I: Suspended structure." *J. Eng. Mech.*, 10.1061/(ASCE)0733-9399(1985)111:4(463), 463–482.

Aktan, A. E., Çatbaş, N., Türer, A., and Zhang, Z. (1998). "Structural identification: Analytical aspects." *J. Struct. Eng.*, 10.1061/(ASCE)0733-9445(1998)124:7(817), 817–829.

Aktan, A. E., et al. (1997). "Structural identification for condition assessment: Experimental arts." *J. Struct. Eng.*, 10.1061/(ASCE)0733-9445(1997)123:12(1674), 1674–1684.

Aydin, M. E., and Fogarty, T. C. (2002). "A modular simulated annealing algorithm for multi-agent systems: A job-shop scheduling application." *Proc., 2nd Int. Conf. on Responsive Manufacturing*, Gaziantep Univ., Gaziantep, Turkey, 318–323.

Azamathulla, H. M., Ghani, A. A., Zakaria, N. A., and Guven, A. (2010). "Genetic programming to predict bridge pier scour." *J. Hydraul. Eng.*, 10.1061/(ASCE)HY.1943-7900.0000133, 165–169.

Behmanesh, I., and Moaveni, B. (2015). "Probabilistic identification of simulated damage on the Dowling Hall footbridge through Bayesian finite element model updating." *Struct. Control Health Monit.*, 22(3), 463–483.

Blum, C., and Roli, A. (2008). "Hybrid metaheuristics: An introduction." *Stud. Comput. Intell.*, 114, 1–30.

Castillo, O., Trujillo, L., and Melin, P. (2007). "Multiple objective genetic algorithms for path planning optimization in autonomous mobile robots." *Soft Comput.*, 11(3), 269–279.

Catbas, F. N., Ciloglu, S. K., Hasancebi, O., Grimmelsman, K., and Aktan, A. E. (2007). "Limitations in structural identification of large constructed structures." *J. Struct. Eng.*, 10.1061/(ASCE)0733-9445(2007)133:8(1051), 1051–1066.

Catbas, F. N., Kijewski-Correa, T., and Aktan, A. E. (2013). *Structural identification of constructed systems: Approaches, methods, and technologies for effective practice of St-Id*, ASCE, Reston, VA.

Chen, D., Lee, C. Y., and Park, C. H. (2005). "Hybrid genetic algorithm and simulated annealing (HGASA) in global function optimization." *Proc., 17th IEEE Int. Conf. on Tools with Artificial Intelligence*, IEEE, Washington, DC, 129–133.

Cheng, A., and Yu, D. (2013). "Genetic algorithm for vehicle routing problem." *Proc., 4th Int. Conference on Transportation Engineering (ICTE)*, ASCE, Reston, VA, 2876–2881.

Cheung, S. H., and Beck, J. L. (2009). "Bayesian model updating using hybrid Monte Carlo simulation with application to structural dynamic models with many uncertain parameters." *J. Eng. Mech.*, 10.1061/(ASCE)0733-9399(2009)135:4(243), 243–255.

Ching, J., Beck, J. L., Porter, K. A., and Shaikhutdinov, R. (2006). "Bayesian state estimation method for nonlinear systems and its application to recorded seismic response." *J. Eng. Mech.*, 10.1061/(ASCE)0733-9399(2006)132:4(396), 396–410.

Ciloglu, K., Zhou, Y., Moon, F., and Aktan, A. E. (2012). "Impacts of epistemic uncertainty in operational modal analysis." *J. Eng. Mech.*, 10.1061/(ASCE)EM.1943-7889(2012)138:9(1059), 1059–1070.

Cross, E. J., Koo, K. Y., Brownjohn, J. M. W., and Worden, K. (2013). "Long-term monitoring and data analysis of the Tamar Bridge." *Mech. Syst. Sig. Process.*, 35(1–2), 16–34.

Dubbs, N. C. (2012). "Development, validation, and assessment of a multiple model structural identification method." Ph.D. thesis, Dept. of Civil Engineering, Drexel Univ., Philadelphia.

Dubbs, N. C., and Moon, F. L. (2016). "Assessment of long-span bridge performance issues through an iterative approach to ambient vibration–based structural identification." *J. Perform. Constr. Facil.*, 10.1061/(ASCE)CF.1943-5509.0000877, 04016029.

Friswell, M. I., and Mottershead, J. E. (1995). *Finite element model updating in structural dynamics*, Kluwer Academic, Dordrecht, Netherlands.

Furuta, H., Nakatsu, K., Ishibashi, K., and Miyoshi, N. (2014). "Optimal bridge maintenance of large number of bridges using robust genetic algorithm." *Proc., Structures Congress 2014*, ASCE, Reston, VA, 2282–2291.

Goldberg, D. E. (1989). *Genetic algorithms in search, optimization and machine learning*, Addition-Wesley, Boston.

Grimmelsman, K. A. (2006). "Experimental characterization of towers in cable-supported bridges by ambient vibration testing." Ph.D. thesis, Dept. of Mechanical Engineering and Mechanics, Drexel Univ., Philadelphia.

Hart, G. C., and Yao, J. T. P. (1977). "System identification in structural dynamics." *J. Eng. Mech. Div.*, 103(6), 1089–1104.

He, X., Moaveni, B., Conte, J. P., Elgamal, A., and Masri, S. F. (2009). "System identification of Alfred Zampa Memorial Bridge using dynamic field test data." *J. Struct Eng.*, 10.1061/(ASCE)0733-9445(2009)135:1(54), 54–66.

Jaishi, B., Kim, H.-J., Kim, M. K., Ren, W.-X., and Lee, S.-H. (2007). "Finite element model updating of concrete-filled steel tubular arch bridge under operational condition using modal flexibility." *Mech. Syst. Sig. Process.*, 21(6), 2406–2426.

Jaishi, B., and Ren, W.-X. (2005). "Structural finite element model updating using ambient vibration test results." *J. Struct. Eng.*, 10.1061/(ASCE)0733-9445(2005)131:4(617), 617–628.

Kirkpatrick, S., Gelatt, C. D., Jr., and Vecchi, M. P. (1983). "Optimization by simulated annealing." *Sci.*, 220(4598), 671–680.

Ko, J. M., and Ni, Y. Q. (2005). "Technology developments in structural health monitoring of large-scale bridges." *Eng. Struct.*, 27(12), 1715–1725.

Koh, C. G., Chen, Y. F., and Liaw, C.-Y. (2003). "A hybrid computational strategy for identification of structural parameters." *Comput. Struct.*, 81(2), 107–117.

Krishnamoorthy, C. S., Venkatesh, P. P., and Sudarshan, R. (2002). "Object-oriented framework for genetic algorithms with application to space truss optimization." *J. Comput. Civ. Eng.*, 10.1061/(ASCE)0887-3801(2002)16:1(66), 66–75.

Kwong, H. S., Lau, C. K., and Wong, K. Y. (1995). "Monitoring system for Tsing Ma Bridge." *Proc., 13th Structures Congress*, Vol. 1, ASCE, Reston, VA, 264–267.

Liu, S. C., and Yao, J. T. P. (1978). "Structural identification concept." *J. Struct. Div.*, 104(12), 1845–1858.

Magalhães, F., Cunha, A., and Caetano, E. (2008). "Dynamic monitoring of a long span arch bridge." *Eng. Struct.*, 30(11), 3034–3044.

Mantawy, A. H., Abdel-Magid, Y. L., and Selim, S. Z. (1998). "A simulated annealing algorithm for unit commitment." *IEEE Trans. Power Syst.*, 13(1), 197–204.

MATLAB [Computer software]. MathWorks, Natick, MA.

Midas [Computer software]. Midas Information Technology, Gyeonggi-do, Korea.

Moon, F. L., and Aktan, A. E. (2006). "Impacts of epistemic (bias) uncertainty on structural identification of constructed (civil) systems." *Shock Vib. Digest*, 38(5), 399–420.

Moon, F. L., Frangopol, D. M., Catbas, F. N., and Aktan, A. E. (2010). "Infrastructure decision-making based on structural identification." *Structures Congress 2010*, ASCE, Reston, VA, 590–596.

Oberkampf, W. L. (2005). "Uncertainty quantification using evidence theory." *Proc., Advanced Simulation and Computing Workshop: Error Estimation, Uncertainty Quantification, and Reliability in Numerical Simulations*, National Nuclear Security Administration (NNSA), Washington, DC.

Pan, Q., Grimmelsman, K. A., Moon, F. L., and Aktan, A. E. (2009). "Mitigating epistemic uncertainty in structural identification." *J. Struct. Eng.*, 10.1061/(ASCE)ST.1943-541X.0000248, 1–13.

PARIS [Computer software]. Tufts Univ., Medford, MA.

Peeters, B., and DeRoeck, G. (1998). "Stochastic subspace system identification of a steel transmitter mast." *Proc., 16th Int. Modal Analysis Conf.*, Society for Experimental Mechanics, Bethel, CT, 130–136.

Phillips, A. W., Allemang, R. J., and Fladung, W. A. (1998). "The complex mode indicator function (CMIF) as a parameter estimation method." *Proc., 16th Int. Modal Analysis Conf.*, Society for Experimental Mechanics, Bethel, CT, 705–710.

Raphael, B., and Smith, I. (1998). "Finding the right model for bridge diagnosis." *Artificial intelligence in structural engineering: Information technology for design, collaboration, maintenance, and monitoring*, Springer, London, 308–319.

Raphael, B., and Smith, I. F. C. (2003). "A direct stochastic algorithm for global search." *Appl. Math. Comput.*, 146(2–3), 729–758.

Ren, W.-X., Zhao, T., and Harik, I. E. (2004). "Experimental and analytical modal analysis of steel arch. bridge." *J. Struct. Eng.*, 10.1061/(ASCE)0733-9445(2004)130:7(1022), 1022–1031.

Robert-Nicoud, Y., Raphael, B., and Smith, I. F. C. (2005). "Configuration of measurement systems using Shannon's entropy function." *Comput. Struct.*, 83(8-9), 599– 612.

Sanayei, M., Khaloo, A., Gul, M., and Catbas, F. N. (2015). "Automated finite element model updating of a scale bridge model using measured static and modal test data." *Eng. Struct.*, 102, 66–79.

SAP2000 [Computer software]. Computers and Structures, Walnut Creek, CA.

Schlune, H., Plos, M., and Gylltoft, K. (2009). "Improved bridge evaluation through finite element model updating using static and dynamic measurements." *Eng. Struct.*, 31(7), 1477–1485.

Shih, C. Y., Tsuei, Y. G., Allemang, R. J., and Brown, D. L. (1988). "Complex mode indication function and its applications to spatial domain parameter estimation." *Mech. Syst. Sig. Process.*, 2(4) 367–377.

Sipple, J. D., and Sanayei, M. (2014). "Finite element model updating using frequency response functions and numerical sensitivities." *Struct. Control Health Monit.*, 21(5), 784–802.

Smith, I. F., and Saitta, S. (2008). "Improving knowledge of structural system behavior through multiple models." *J. Struct. Eng.*, 10.1061/(ASCE)0733-9445(2008)134:4(553), 553–561.

Sonmez, R., and Bettemir, Ö. H. (2012). "A hybrid genetic algorithm for the discrete time-cost trade-off problem." *Expert. Syst. Appl.*, 39(13), 11428–11434.

Strand7 [Computer software]. Strand7 Pty., Sydney, NSW, Australia.

Sun, H., and Betti, R. (2015). "A hybrid optimization algorithm with Bayesian inference for probabilistic model updating." *Comput.-Aided. Civ. Infrastruct. Eng.*, 30(8) 602–619.

Sun, H., Luş, H., and Betti, R. (2013). "Identification of structural models using a modified artificial bee colony algorithm." *Comput. Struct.*, 116, 59–74.

Sun, H., Mordret, A., Prieto, G. A., Toksöz, M. N., and Büyüköztürk, O. (2017). "Bayesian characterization of buildings using seismic interferometry on ambient vibration." *Mech. Syst. Sig. Process.*, 85, 468–486.

Wan, H.-P., and Ren, W.-X. (2015). "A residual-based Gaussian process model framework for finite element model updating." *Comput. Struct.*, 156, 149–159.

Wang, G. S. (2009). "Application of hybrid genetic algorithm to system identification." *Struct. Control Health Monit.*, 16(2), 125–153.

Yu, S., and Ou, J. (2016). "Structural health monitoring and model updating of Aizhai suspension bridge." *J. Aerosp. Eng.*, 10.1061/(ASCE)AS.1943-5525.0000653, B4016009.

Zhang, J., Prader, J., Grimmelsman, K. A., Moon, F. L., Aktan, A. E., and Shama, A. (2013a). "Experimental vibration analysis for structural identification of a long-span suspension bridge." *J. Eng. Mech.*, 10.1061/(ASCE)EM.1943-7889.0000416, 748–759.

Zhang, J., Wan, C., and Sato, T. (2013b). "Advanced Markov chain Monte Carlo approach for finite element calibration under uncertainty." *Comput.-Aided. Civ. Infrastruct. Eng.*, 28(7), 522–530.

Zhong, S. T. (2003). *The concrete-filled steel tubular structures*, Tsinghua University Press, Beijing.

Zhou, Y. (2008). "Parameter identification experiment and research on elastic foundation slab and reinforced concrete frame structure." Ph.D. thesis, College of Civil Engineering, Hunan Univ., Changsha, Hunan, China.

Zhu, G., and Kwong, S. (2010). "Gbest-guided artificial bee colony algorithm for numerical function optimization." *Appl. Math. Comput.*, 217(7), 3166–3173.